frontiers | Frontiers in Water

TYPE Brief Research Report
PUBLISHED 23 July 2025
DOI 10.3389/frwa.2025.1617212

OPEN ACCESS

EDITED BY
Yuan Li,
Shaanxi Normal University, China

REVIEWED BY
Michael Nones,
Institute of Geophysics, Polish Academy of Sciences, Poland
Haibo Yang,
Zhengzhou University, China
Longfei Wang,
Hohai University, China
Wenchuan Wang,
North China University of Water Resources and Electric Power, China

*CORRESPONDENCE
Fuxin Chai
✉ chaifx@iwhr.com
Shilong Hao
✉ haoshilong24@163.com

RECEIVED 24 April 2025
ACCEPTED 04 July 2025
PUBLISHED 23 July 2025

CITATION
Li T, Hao S, Chai F, Li K and Tong H (2025) Comparative analysis of different hydrological models in flood forecasting for the upper Juma River basin.
Front. Water 7:1617212.
doi: 10.3389/frwa.2025.1617212

Comparative analysis of different hydrological models in flood forecasting for the upper Juma River basin

Ting Li[1], Shilong Hao[1]*, Fuxin Chai[2]*, Kuang Li[2] and Haoqiang Tong[1]

[1]School of Geomatics and Geographic Information, North China University of Water Resources and Electric Power, Zhengzhou, China, [2]China Institute of Water Resources and Hydropower Research, Beijing, China

Accurate flood forecasting is of critical importance for flood control and disaster mitigation. This study focuses on the upper basin of the Juma River and employs the China Flash Flood Hydrological Model (CNFF) to calibrate model parameters using three specific runoff generation models implemented within the CNFF platform: the Xin'anjiang three-source saturation-excess runoff model, the vertical mixed runoff model, and the Dahuofang model. These models, respectively, represent three distinct physical runoff mechanisms—saturation-excess, vertical mixing, and infiltration-excess. The primary scientific objective is to systematically compare the flood forecasting accuracy of these models and to identify the most suitable one for flood forecasting in this basin. The results indicate that the overall forecasting accuracy of the Xin'anjiang model is superior to that of the vertical mixed runoff model and the Dahuofang model. The absolute value of the relative error in peak discharge and the relative error in mean runoff depth simulated by the Xin'anjiang model are 6.8 and 10.7%, respectively. The absolute value of the mean peak arrival time error is 0.47 h, and the average Nash-Sutcliffe efficiency coefficient is 0.69. The Xin'anjiang model demonstrated superior performance, achieving an average Nash-Sutcliffe Efficiency (NSE) approximately 0.21 higher than the other models across the evaluated events. When flood discharge is high and exhibits a single-peak pattern, the simulation performance of all runoff models improves. Overall, the Xin'anjiang model achieves a Class B accuracy level in flood simulation for the upper Juma River basin. These findings provide a reference for hydrological simulation, flood forecasting, and early warning in the upper Juma River basin.

KEYWORDS

China flash flood hydrological model, Xin'anjiang model, vertical mixed runoff model, Juma River, flood forecasting

1 Introduction

Flood disasters have become a key risk factor constraining regional sustainable development (Birkmann et al., 2015; Mai et al., 2020; Rehman et al., 2019; Ran and Nedovic-Budic, 2016; Sam et al., 2021; Kimuli et al., 2021; Wang et al., 2024; Wang et al., 2021). As one of the country's most sensitive to monsoonal climate responses, China suffered direct economic losses of up to 128.899 billion yuan due to flood-related disasters in 2022, accounting for 54.01% of the total losses caused by disasters resulting from natural hazards (Compilation group of China Flood and Drought Disaster Prevention Bulletin, 2023; Kundzewicz et al.,

2020; Zhang and Wang, 2022; Duan et al., 2016). Extreme events such as the record-breaking rainstorm in Henan Province on July 20, 2021 (daily precipitation reaching 624.1 mm) (Zhao et al., 2023; Chen et al., 2023; Nie and Sun, 2022), and the large-scale flood in the Haihe River Basin in 2023 (Lan and Wang, 2025) (peak discharge of the Juma River surpassing the 1963 record) underscore the urgent need for accurate flood forecasting. Flood forecasting plays a crucial role in mitigating the impacts of flood disasters (Emerton et al., 2016; Wee et al., 2023; Kumar et al., 2023). Hydrological models are essential tools for flood forecasting (Grimaldi et al., 2019; Qi et al., 2021; Kumar et al., 2023); however, due to differences in hydrological mechanisms and regional hydro-climatic characteristics, the applicability of different hydrological models varies across watersheds (Xu, 2010). Therefore, a comparative analysis of different model structures is crucial for identifying the most appropriate model for a specific basin," which directly leads into our study's objective (Jain et al., 2018; Chen et al., 2016; Awol et al., 2021).

At present, a large body of research has focused on using different hydrological models for flood forecasting in various watersheds. For example, in the Tunxi watershed of southern Anhui Province, the Xin'anjiang model and the API-Nash model have been used for flood event simulations. Under limited parameter conditions, the API-Nash model demonstrated sufficient accuracy to meet the requirements of flash flood forecasting (Ye et al., 2012). In the Shuangqiao watershed of the Pearl River system, Zhu and Zhou (2016) conducted a comparative analysis of the Xin'anjiang model, TOPMODEL, and BTOPMC model in terms of simulation accuracy and adaptability in small watersheds. The Juma River, one of the main tributaries of the Daqing River system within the Haihe River Basin, is not only a critical area affected by flooding in the basin but also the core region of the large-scale flood event on July 23, 2023. The Upper Juma River Basin, characterized by its steep topography, flashy flood responses typical of mountainous catchments, and increasing vulnerability due to localized intense rainfall events in recent years, presents a significant challenge for operational flood forecasting. Identifying the most suitable hydrological model for the Juma River is therefore of great significance to enhancing flood forecasting capabilities in the Haihe River Basin. Some scholars have already applied individual hydrological models to study the Daqing River Basin. For example, Ma et al. (2024) utilized the domestically developed distributed hydrological model SKY-HydroSAT to analyze runoff generation during the "7·23" flood event. Che (2024) used the Xin'anjiang model for calibration of moderate and large flood events in the Zijingguan watershed. However, research on the Juma River Basin has predominantly focused on the application of single models, with a lack of systematic comparative analysis among different hydrological models.

To address this gap, the China Institute of Water Resources and Hydropower Research developed a distributed hydrological model known as the China Flash Flood Hydrological Model (CNFF), based on runoff generation and confluence characteristics across various climate zones in China. This model is built upon a large-scale distributed framework and detailed geomorphological data, with simplified parameterization that can be largely determined using the national small watershed basic dataset. It is particularly suited for simulating and forecasting flash floods in small and medium-sized watersheds with limited data, and has been widely used in China for rainstorm and flash flood warning applications (Chen et al., 2025; Zhai et al., 2021; Zhai et al., 2021; Zhai et al., 2020; Wang et al., 2023). In this study, the CNFF framework operates at the sub-watershed scale, with the sub-watershed delineation based on DEM analysis and hydrological characteristics, providing a spatial discretization foundation for distributed modeling. We selected the Xinanjiang model, the vertical exchange model, and the DahuoFang model to simulate multiple flood events in the upper reaches of the Juma River basin, and conducted a comparative analysis of the simulation accuracy and adaptability of the three models. The aim of this study is to provide a scientific basis for improving flood forecasting capability in the Juma River basin, and to offer useful insights for optimizing and improving flood forecasting systems in small and medium-sized watersheds nationwide. These three models were chosen because they represent three key runoff generation mechanisms: saturation-excess runoff (Xinanjiang model), where runoff occurs after soil moisture capacity is saturated; infiltration-excess runoff (DahuoFang model), where runoff is generated when rainfall intensity exceeds the soil infiltration capacity; and vertical water exchange (vertical exchange runoff model), which focuses on the vertical interaction between soil water and groundwater. By comparing these three models, we aim to diagnose which physical process dominates flood formation in the semi-humid mountainous area with thin soil layers in the Juma River basin.

2 Materials and methods

2.1 General situation of the research region

The Juma River is a key tributary of the Daqing River system within the Haihe River Basin. It originates from the southern foothills of Qishan Mountain in Laiyuan County, Hebei Province. Its headwaters are characterized by the emergence of surface runoff from a cluster of underground springs. The river flows generally from northwest to southeast and bifurcates into two branches at Tiesuoya in Laishui County, Baoding City, Hebei Province. The southern branch, known as the South Juma River, continues to flow within Hebei Province, while the northern branch, referred to as the North Juma River, passes through Laishui County (Hebei), Fangshan District (Beijing), and Zhuozhou City (Hebei), eventually discharging into the Baiyangdian water system. The geographical location of the study area is shown in Figure 1.

The Juma River Basin exhibits hydrometeorological characteristics typical of rivers in northern monsoon regions. The average annual precipitation ranges from 550 to 650 mm, with approximately 70% falling during the flood season from June to September. The average annual temperature is between 11°C and 13°C. According to observational data from the Zijingguan Hydrological Station (1955–2019), the basin's average annual runoff is approximately 1.56 billion cubic meters, with a significant proportion contributed by baseflow. Runoff distribution is highly uneven across seasons, with over 60% occurring in summer (June to August), while winter often experiences flow interruptions. Flood events in the basin are characterized by sharp rises and falls in discharge. The historical maximum peak flow has reached 10,000 m^3/s. During the extraordinary flood event of July 2023 ("7·23" event), the runoff coefficient at Zhangfang Station reached 0.40, surpassing historical records and highlighting the basin's

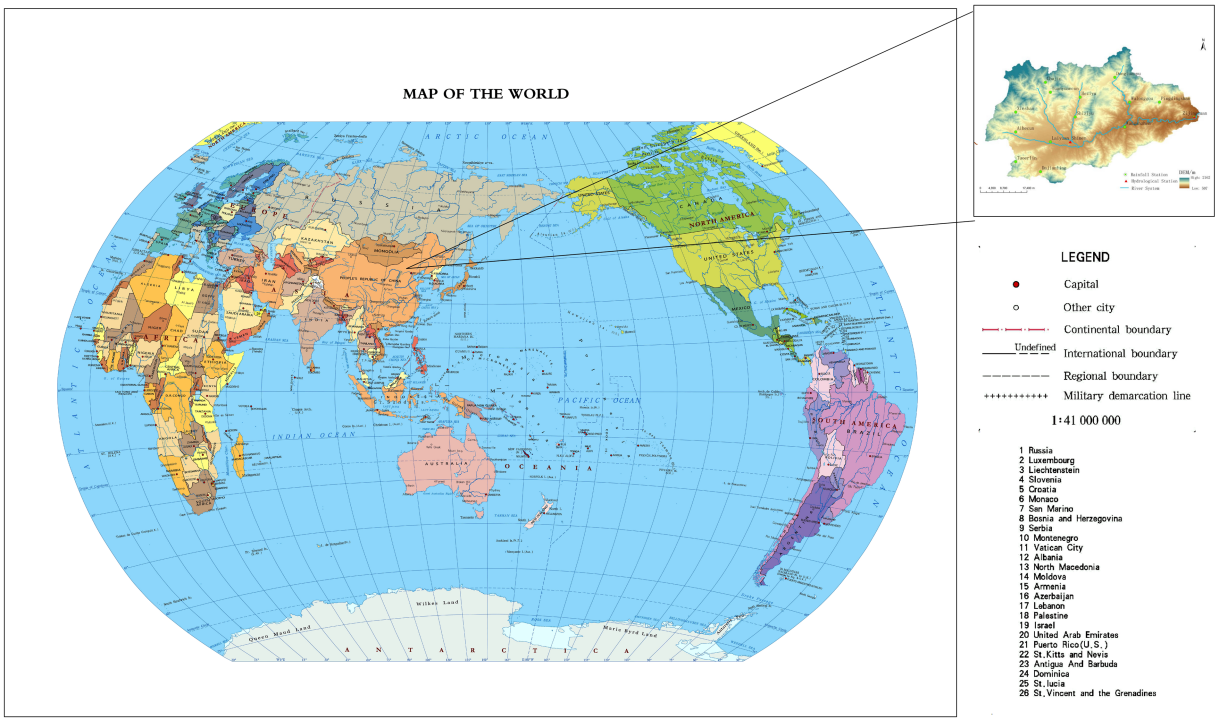

FIGURE 1
Location map of the study area.

hydrological sensitivity under extreme climatic conditions. Under the influence of global climate change, recent observations indicate a marked increase in the frequency of extreme precipitation events within the basin. From 2010 to 2020, the number of heavy rainfall days increased by 23% compared to the baseline period (1961–1990), exacerbating flood risk and intensifying pressure on flood management. This study focuses on the upstream region of the Juma River above the Zijingguan Hydrological Station. The area is located within a temperate continental monsoon climate zone and is characterized by distinct seasonal variation. Summers are typically hot and humid, whereas winters are cold and dry.

2.2 Data collection and processing

The fundamental data used in this study comprise two main categories: geographic information data and rainfall–runoff event data. The geographic information data primarily include the Digital Elevation Model (DEM), river network distribution, land use types, and soil texture. All datasets were obtained from the National Geomatics Center of China.[1] Standard pre-processing, including resampling of DEM and soil texture data to a consistent spatial resolution and reclassification of land use categories to match model input requirements, was performed to ensure compatibility with the CNFF model structure. Within the study basin, 14 rainfall stations and 2 hydrological stations are installed. Due to insufficient data availability at the Shimen Hydrological Station, this study selects the Zijingguan Hydrological Station as the forecast section. The Zijingguan (River) Station serves as the control point for the Zijingguan section, with a controlled drainage area of 1868.47 km^2. The basin's topographic features and the spatial distribution of monitoring stations are illustrated in Figure 2. The hydrological data for the Zijingguan section are derived from observed records, which have been compiled and verified, ensuring high reliability. Hourly rainfall data from 14 rainfall stations—including Xieshan, Aihecun, Laiyuan, Chajin, Tuanyuancun, Huziyu, Shiziyu, Shimen, Dongtuanpu, and Wulonggou—were collected for the period 1955–2019. Additionally, flood event records for the Zijingguan section were compiled. From these, seven representative flood events were selected for model parameter calibration. These seven historical flood events were selected for model calibration to represent a diverse range of hydrological conditions, including varying flood magnitudes (from small to large peak discharges and runoff volumes), different seasons within the typical flood period of the basin, and distinct antecedent rainfall patterns. This selection aims to ensure robust parameterization and comprehensive model evaluation.

2.3 Model evaluation

To evaluate the accuracy of flood forecasting, fur key indicators are employed: Relative Error of Runoff Depth (RER), Relative Error of Peak Discharge (REQ), Peak Time Error (TP), and the Nash–Sutcliffe Efficiency Coefficient (NSE) (Mathevet et al., 2006). The optimal values for RER, REQ, and TP are 0, while the optimal value for SNSE is 1. In model performance evaluation,

1 https://www.ngcc.cn

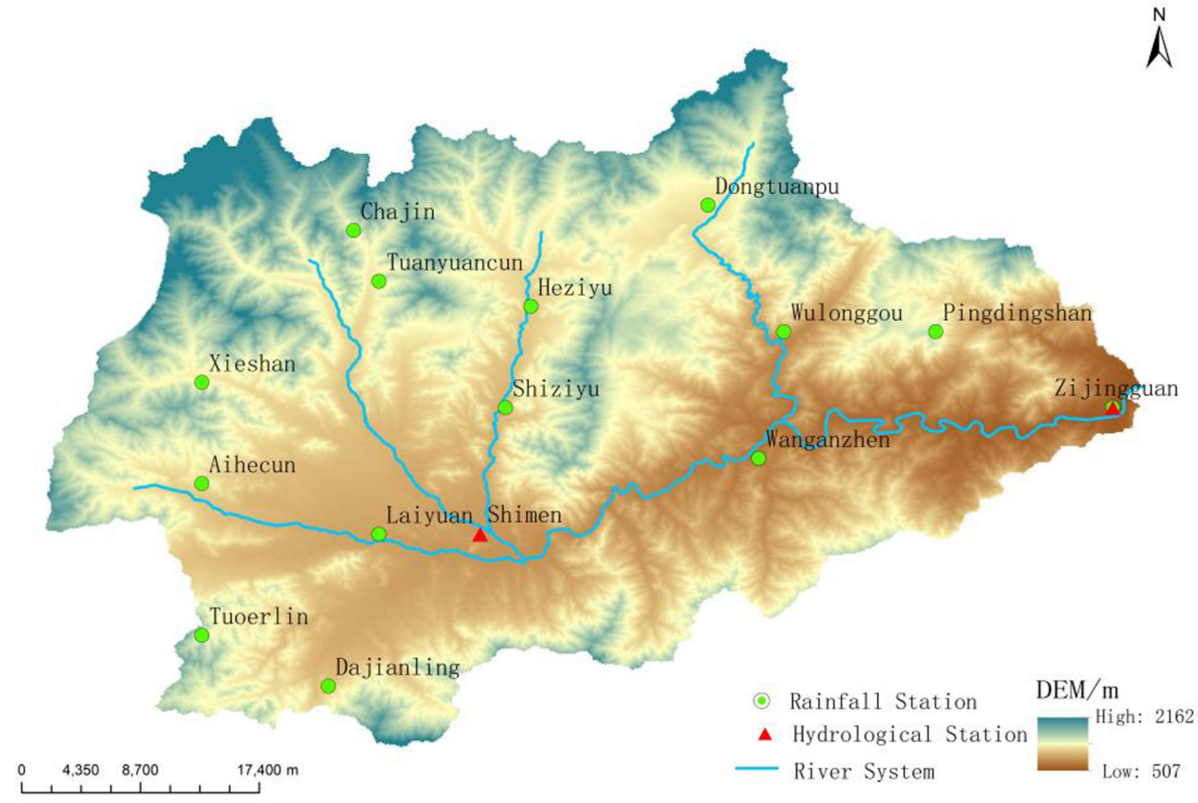

FIGURE 2
Topographic map and distribution of monitoring stations in the upper Juma River basin.

simulation results are considered acceptable when the absolute values of RER and REQ are within 20%, TP is within ±2 h, and SNSE exceeds 0.6. The calculation formulas for these indicators are as follows:

$$RER = \frac{|Rs - Ro|}{Ro} \quad (1)$$

$$REQ = \frac{|Qs - Qo|}{Qo} \quad (2)$$

$$TP = Ts - To \quad (3)$$

$$NSE = 1 - \frac{\sum_{i=1}^{n}\left[Qs(i) - Qo(i)\right]^2}{\sum_{i=1}^{n}\left[Qo - \overline{Qo}\right]^2} \quad (4)$$

Where Rs is the simulated runoff depth (mm); Ro is the observed runoff depth (mm); Qs is the simulated peak discharge (m^3/s); Qo is the observed peak discharge (m^3/s); Ts is the simulated time to peak (h); To is the observed time to peak (h); $Qs(i)$ is the simulated discharge at time step i (m^3/s); $Qs(i)$ is the observed discharge at time step i (m^3/s); $\overline{Qo}$ is the mean observed discharge (m^3/s); and n is the length of the flood event time series.

Accuracy Grading: Based on the 'Specifications for Hydrological Forecasting Information' (GB/T 22482–2008), flood forecast accuracy is categorized to standardize performance evaluation. For key indicators such as the Relative Error of Peak Discharge (REQ) and Relative Error of Runoff Depth (RER), a forecast is typically classified as follows:

Class A (Excellent): If the absolute relative error is £ 20%

Class B (Good): If the absolute relative error is between 20 and 40%

Class C (Acceptable): If the absolute relative error is between 40 and 50%

For the Peak Time Error (TP), a forecast within ±2 h of the observed peak is generally considered to meet high-grade accuracy requirements (i.e., Class A). This framework is now introduced early in our methodology and is used consistently to interpret model performance in the Results and Discussion sections.

2.4 Model configuration method

Taking the upper reaches of the North Juma River Basin as the research object, the runoff generation, runoff concentration, evaporation, and river channel evolution patterns of each model are shown in the following table (see Table 1), the use of a 'Three-layer Evaporation' module in the Xin'anjiang model versus a 'Daily Average Evaporation' in the other two reflects a key structural difference in how

soil moisture dynamics are accounted for. Conversely, employing the 'Dynamic Muskingum Method' for river routing in all three models ensures consistency in the confluence process, allowing our comparison to focus primarily on the differences in the runoff generation modules.

2.5 Parameter calibration

The parameters of each of the three hydrological models were optimized using a multi-event joint calibration approach, which involved simultaneously utilizing seven representative flood events (see Table 2) to identify a single, robust parameter set that best captures the overall rainfall-runoff characteristics of the upper Juma River basin. The calibration process was conducted by manually adjusting the parameters to maximize the Nash–Sutcliffe efficiency (NSE) and minimize errors in runoff depth and peak discharge across all seven flood events. The final optimized parameter values for each model are presented in Tables 3–5. All the calibrated parameter values fall within the physically reasonable range for similar climatic regions, confirming the reliability of the calibration results. The key parameters of each model are described in the following sections.

2.5.1 Xin'anjiang model parameters

The Xin'anjiang model is characterized by parameters that describe the basin's water storage capacity and runoff generation process (see Table 3). The key parameters include:

TABLE 1 Configuration methods of each model.

Mode	Runoff generation module	Runoff concentration module	Evaporation module	River flood routing module
Xin'anjiang model	Three-source full storage runoff generation method	Standardized unit hydrograph	Three - layer evaporation	Dynamic Muskingum method
Vertical mixed runoff generation model	Vertical mixed runoff generation method	Standardized unit hydrograph	Daily average evaporation	Dynamic Muskingum method
Dahuofang model	Dahuofang method	Standardized unit hydrograph	Daily average evaporation	Dynamic Muskingum method

TABLE 2 Historical flood events table of the Zijingguan section.

Flood number	Start and end time	Rainfall amount (mm)	Peak flood (m^3/s)	Peak–arrival time	Volume of flood ($106m^3$)
19550817	1955/8/15 12–8/20 12	223.1	2020	1955/8/17 5	208.661
19590806	1959/8/3 0–8/8 21	164.2	648	1959/8/6 16	114.57
19630808	1963/8/3 4–8/9 21	426.2	4,490	1963/8/8 6	440.029
20060630	2006/6/28 20–7/1 0	33.7	56.5	2006/6/30 2	1.951
20110825	2011/8/24 9–8/31 3	72.6	109	2011/8/25 16	6.868
20120721	2012/7/21 9–7/25 8	174	2156.349	2012/7/21 21	73.376
20160720	2016/7/19 11–7/24 0	122.1	113.2	2016/7/20 18	15.281

TABLE 3 Parameters of the Xin'anjiang Model for the Zijingguan section.

Parameter symbol	Parameter name	Parameter value
B	Exponent of the storage capacity curve	0.2
IMP	Impervious area ratio	0.01
WUM	Upper layer soil storage capacity	20
WLM	Lower layer soil storage capacity	70
WDM	Deep layer soil storage capacity	45
EX	Exponent of the free water storage curve	1.1
SM	Free water storage capacity	45
KS	Daily outflow coefficient of interflow	0.67
KG	Daily outflow coefficient of groundwater runoff	0.2
KKS	Daily recession coefficient of interflow	0.5
KKG	Daily recession coefficient of groundwater runoff	0.1
KC	Evapotranspiration conversion coefficient of the basin	0.95
C	Deep evapotranspiration diffusion coefficient	0.11

TABLE 4 Parameters of the vertical mixed runoff generation model for the Zijingguan section.

Parameter symbol	Parameter name	Parameter value
IMP	Impervious area ratio	0.01
B	Exponent of the storage capacity distribution curve	0.3
WUM	Upper layer soil water storage capacity	20
WLM	Middle layer soil water storage capacity	80
WDM	Deep layer soil water storage capacity	40
K	Decay coefficient of Horton infiltration capacity	0.08
F0	Average initial maximum infiltration capacity of the basin	10
Fc	Average steady infiltration capacity of the basin	4
BX	Exponent of the infiltration capacity distribution curve	0.5
DW	Permissible error of soil moisture content	0.01
KS	Daily outflow coefficient of interflow	0.5
KG	Daily outflow coefficient of groundwater runoff	0.2
KKS	Daily recession coefficient of interflow	0.1
KKG	Daily recession coefficient of groundwater runoff	0.1

TABLE 5 Parameters of the Dahuofang model for the Zijingguan section.

Parameter symbol	Parameter name	Parameter value
IMP	Impervious area ratio	0.01
S0	Surface storage capacity	30
a	Shape parameter of the surface storage capacity distribution curve	4
U0	Lower layer storage capacity	80
V0	Groundwater reservoir storage capacity	40
B	Shape parameter of the parabolic infiltration distribution curve	2
K2	Curvature coefficient of the lower layer infiltration curve	0.5
Kw	Ratio of groundwater runoff to groundwater reservoir infiltration intensity	0.8

WUM, WLM, WDM: These represent the water storage capacity (in mm) of the upper, lower, and deep soil layers, respectively. They collectively define the total water holding capacity of the basin's soil profile before runoff is generated.

B: The exponent of the storage capacity distribution curve, which describes the spatial variability of soil water storage capacity across the basin.

IMP: The fraction of the basin area that is impervious, directly contributing to surface runoff.

KC: The coefficient relating pan evaporation to potential evapotranspiration, which governs water loss from the basin.

KG, KS: The outflow coefficients for interflow and groundwater, respectively. They control the recession rate of these two runoff components.

2.5.2 Vertical mixed runoff model parameters

This model focuses on vertical water movement and infiltration (see Table 4). Its key parameters are:

WUM, WLM, WDM: Similar to the Xin'anjiang model, these define the water storage capacities (in mm) of the upper, middle, and deep soil layers.

Fc: The final, steady-state infiltration capacity of the soil (in mm/h), representing the maximum rate at which water can enter the soil after prolonged wetting.

F0: The initial maximum infiltration capacity of the basin (in mm/h), which is typically higher than Fc and decreases as the soil becomes wetter.

K: The decay coefficient of the Horton infiltration curve, which describes how quickly the infiltration rate decreases from F0 to Fc.

IMP: The impervious area ratio.

2.5.3 Dahuofang model parameters

The Dahuofang model is a lumped model primarily based on the infiltration-excess concept (see Table 5). The key parameters include:

SO: The surface storage capacity (in mm), representing the initial abstractions such as depression storage before runoff begins.

U0, V0: The initial storage capacity (in mm) of the lower layer soil moisture and the groundwater reservoir, respectively.

a: The shape parameter of the surface storage capacity distribution curve, describing its spatial variability.

B: The shape parameter of the parabolic infiltration distribution curve, which reflects the spatial heterogeneity of infiltration capacity.

K2: The curvature coefficient of the lower layer infiltration curve, which influences how rainfall is partitioned between surface runoff and infiltration.

IMP: The impervious area ratio.

10.3389/frwa.2025.1617212

TABLE 6 Comparative analysis of simulation accuracy for different models across various flood events.

No.	Flood number	Nash-Sutcliffe Efficiency (NSE)			Relative error in runoff depth (%)			Relative error in peak discharge (%)			Peak timing error(h)			Pass/Fail		
		XAJ	VMM	DHF	XAJ	VMM	DHF	XAJ	VMM	DHF	XAJ	VMM	DHF	XAJ	VMM	DHF
1	19550817	0.75	0.61	0.65	2.3	−10.9	−17.5	−0.6	6.8	−4.3	0.8	0.8	1.8	Pass	Pass	Pass
2	19590806	0.69	0.55	−0.56	−14.4	−1.4	−32.7	5.8	−0.3	25.2	0	0	1	Pass	Pass	Fail
3	19630808	0.85	0.79	0.71	19.9	15.8	27.7	−1.8	9.8	15.5	0.5	0.5	0.5	Pass	Pass	Fail
4	20060630	0.64	0.6	0.63	−8	−2.7	−11.5	−12.4	9.6	−33.4	0	2	−3	Pass	Pass	Fail
5	20110825	0.26	0.05	0.16	−12.8	−34.1	−26.1	−11.1	−13.6	−16.6	1	−1	−1	Fail	Fail	Fail
6	20120721	0.9	0.76	0.73	−0.3	−27.8	6.8	−3.4	−14.5	12.9	0	0	0	Pass	Fail	Pass
7	20160720	0.75	−0.01	0.53	16.7	−49.1	2	−12.6	−56.6	−4.8	1	−2	2	Pass	Fail	Fail
	Mean	0.69	0.48	0.41	10.6	20.3	17.8	6.8	15.9	16.1	0.47	0.9	1.33			
	Range	0.64	0.8	1.29	34.3	64.9	60.4	18.4	66.4	58.6						
	Qualification rate				86%	57%	57%	100%	86%	71%	100%	100%	86%			

3 Results

3.1 Comparison of forecast accuracy

The simulation results of seven selected flood events using three hydrological models—Xinanjiang (XAJ), Vertical Mixed Runoff Generation (HHC), and Dahuofang (DHF)—were evaluated based on four key performance indicators defined by Equations (1–4) described in Section 2.3. Table 6 provides a comprehensive summary of this comparative analysis. For each flood event and each model, the table presents the Nash-Sutcliffe Efficiency (NSE), the Relative Error in Runoff Depth (RER, in %), the Relative Error in Peak Discharge (REQ, in %), and the Peak Timing Error (TP, in hours). Furthermore, based on the accuracy criteria outlined in our methodology, a "Pass/Fail" assessment is provided for each indicator to quickly evaluate whether the simulation meets the operational forecasting standards. A "Pass" indicates that the result falls within the acceptable range (e.g., $|REQ| \leq 20\%$ and $|TP| \leq 2$ h for Class A). The following subsections provide a detailed analysis and discussion of these results, assessing the overall performance, stability, and applicability of each model for flood forecasting in the Upper Juma River Basin.

3.2 Simulation accuracy assessment

3.2.1 Efficiency coefficient

Among the seven flood events simulated in the upper Juma River Basin, the average Nash–Sutcliffe efficiency coefficients for the Vertical Mixed Runoff Generation Model and the Dahuofang Model were 0.48 and 0.41, respectively. In contrast, the Xin'anjiang Model achieved a higher average efficiency coefficient of 0.69, representing an improvement of 0.21 over the other two models. Moreover, the Vertical Mixed Model and the Dahuofang Model exhibited greater event-to-event variability (i.e., a wider range and standard deviation) in their efficiency coefficients across the seven flood events, indicating lower predictive stability compared to the Xin'anjiang model. These results demonstrate that, in terms of fitting the flood hydrograph, the Xin'anjiang Model outperforms the other two models.

3.2.2 Relative error of runoff depth

According to the flood forecasting accuracy evaluation criteria, analysis of the seven simulated flood events revealed that the Vertical Mixed Model and the Dahuofang Model each achieved a compliance rate of 57%, while the Xin'anjiang Model reached a significantly higher compliance rate of 86%. This indicates better applicability of the Xin'anjiang Model for flood forecasting. Additionally, the average and range of RER for the Xin'anjiang Model were both lower and more concentrated compared to the other two models, suggesting superior performance in simulating runoff depth.

3.2.3 Relative error of peak discharge

The Dahuofang Model achieved a 71% compliance rate for peak discharge simulation, meeting Class B accuracy requirements. In comparison, the Vertical Mixed Model and the Xin'anjiang Model achieved compliance rates of 86 and 100%, respectively, both meeting Class A standards. Furthermore, the Xin'anjiang Model exhibited the smallest average and range of peak discharge errors, indicating higher accuracy and overall superiority in peak discharge simulation.

3.2.4 Peak time error

Both the Xin'anjiang Model and the Vertical Mixed Model achieved 100% compliance in simulating peak arrival time, while the Dahuofang Model achieved 86%. Overall, all three models met the Class A standard in this category. However, a comparison of average peak time errors shows that the Xin'anjiang Model provides higher simulation accuracy for peak timing than the other two models. This high accuracy in predicting flood peak timing, particularly the 100% compliance for TP (within ±2 h) by the Xin'anjiang and VMM models and an average error of only 0.47 h for Xin'anjiang, is crucial for effective flood warning and timely emergency response, significantly enhancing the operational value of these models.

The Xin'anjiang Model achieved an average compliance rate of 95.3% across the three primary forecast indicators—peak discharge, runoff depth, and peak time—meeting Class A accuracy standards. In contrast, the Vertical Mixed Model and the Dahuofang Model achieved average compliance rates of 81 and 71.3%, respectively, both corresponding to Class B accuracy. Based on a comprehensive analysis of the four evaluation indicators defined in the flood forecasting accuracy methodology, the Xin'anjiang Model achieves an overall Class A performance in simulating floods in the upper Juma River Basin. Although the Vertical Mixed Model and the Dahuofang Model performed relatively well in simulating peak arrival time, their lower compliance rates for the remaining indicators indicate limited reliability. Therefore, the Xin'anjiang Model is considered the most suitable option for flood simulation in this basin and is recommended as the preferred comprehensive model.

3.3 Comparison of individual flood events

Selected flood events are presented to illustrate the model performance under different flood types. The event on August 17, 1955 (19550817) is used as an example of a large flood with a double peak; the event on August 8, 1963 (19630808) represents an extraordinary flood with a double peak; the event on July 21, 2012 (20120721) demonstrates a large flood with a single peak; and the event on July 20, 2016 (20160720) serves as an example of a small flood with a double peak. The observed and simulated hydrographs for these events are shown in Figure 3.

Overall, the simulation performance was better for large flood events and poorer for small floods. As flood magnitude increased, the simulation accuracy for single-peak floods improved. However, for the flood event on July 20, 2016, all three models exhibited a delayed peak time, which is consistent with the findings of Zhai et al. (2020), who reported that under varying rainfall intensities—from moderate rain to extremely heavy rain—the average flood peak appeared earlier and the passing rate of the determinacy coefficient improved, indicating a significant enhancement in simulation performance. Nonetheless, under moderate rainfall conditions, the CNFF model still exhibited a certain degree of delay in simulating the peak time. Among the three models, the Xin'anjiang model showed superior simulation results compared to the Vertical Mixed Runoff Generation Model and the Dahuofang Model. In summary, the Xin'anjiang model demonstrates higher simulation accuracy and is more suitable for application in the upper reaches of the Juma River compared to the other two models.

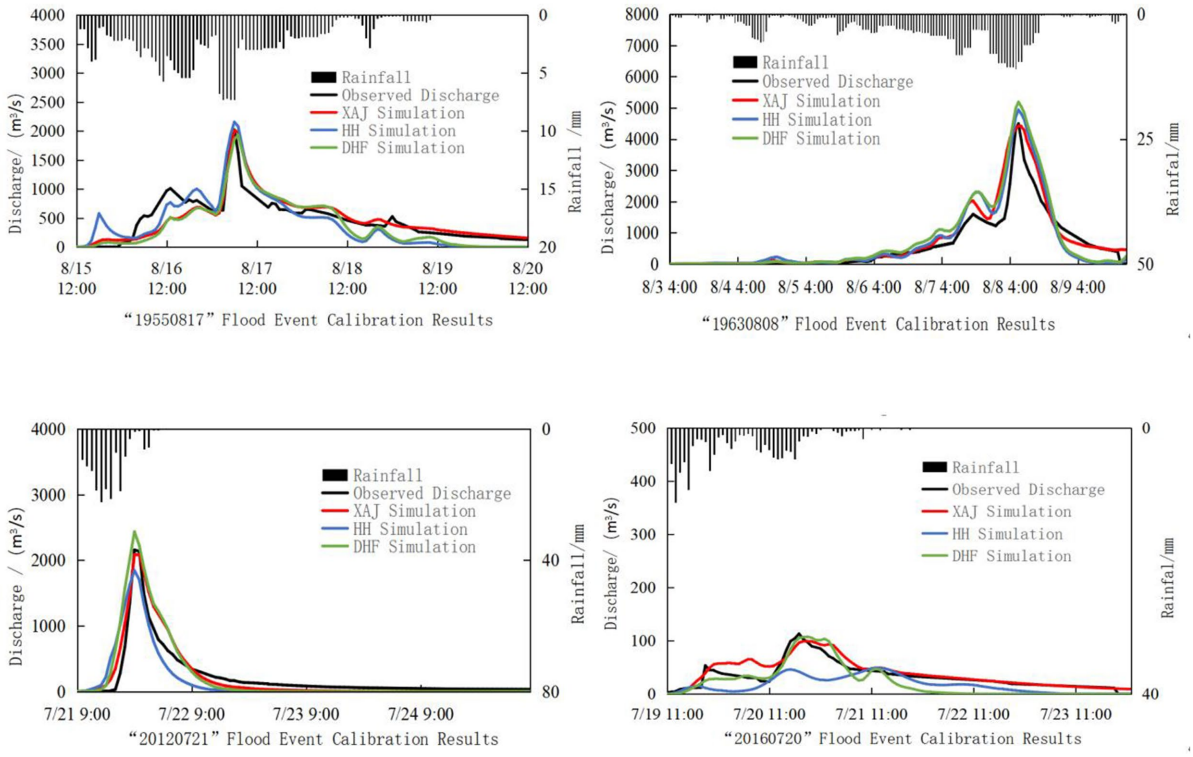

FIGURE 3
Comparison of observed and simulated flood discharges for three hydrological models.

4 Discussion

4.1 Applicability of the Xin'anjiang model

The study demonstrates that the flood simulation results of the Xin'anjiang model show a high degree of agreement with observed data in the upper reaches of the Juma River, confirming its applicability in the semi-arid to semi-humid mountainous regions of northern China. This finding, which confirms the applicability of the Xin'anjiang model in this basin, is consistent with the results of Che (2024). The upper Juma River basin is characterized by a temperate continental monsoon climate, with a flood season that is concentrated between June and September. Precipitation predominantly occurs in the form of heavy rainfall. The region has shallow soil layers with limited water storage capacity, a deep groundwater table, and a low contribution from baseflow. The Xin'anjiang model is based on the saturation-excess runoff generation mechanism, wherein rainfall generates surface runoff only after the soil becomes saturated (Lu, 2021; Jin et al., 2022; Ren-Jun, 1992). This model utilizes a "runoff yield capacity curve" to simulate the soil saturation process, effectively capturing runoff generation following rapid soil saturation. Given the shallow soil and low water retention capacity of the Juma River basin, even moderate rainfall can quickly saturate the soil, triggering saturation-excess runoff. This characteristic enables the Xin'anjiang model to accurately capture the key processes of rainfall-runoff transformation, thereby improving flood forecasting accuracy in the region.

4.2 Inapplicability of the vertical mixed runoff generation model

The Vertical Mixed Runoff Generation Model focuses on simulating vertical water exchange between the soil and groundwater, making it more suitable for regions with significant baseflow contributions. However, the Juma River basin has a deep groundwater table and a negligible baseflow contribution (<10%). The model's emphasis on vertical processes results in underestimation of surface runoff. Moreover, it typically assumes sufficient soil infiltration capacity and neglects the infiltration-excess runoff mechanism. During intense rainfall events, this leads to an underestimation of runoff volumes. For example, during the 20,120,721 flood event, characterized by high rainfall intensity, the model significantly underestimated peak discharge compared to observed values, indicating its inability to accurately simulate flood responses under high-intensity rainfall. This shortcoming demonstrates that the model is not suitable for the Juma River basin or similar mountainous regions in northern China, particularly under extreme precipitation conditions.

4.3 Inapplicability of the Dahuofang model

The Dahuofang Model is centered on the infiltration-excess mechanism, where surface runoff is generated only when rainfall intensity exceeds soil infiltration capacity. This mechanism performs well in regions with thick soils and high water retention capacity. However, in the Juma River basin, soil often becomes saturated after continuous rainfall, meaning that even moderate rainfall can produce runoff via the saturation-excess mechanism. The Dahuofang Model fails to represent this process. When the soil is unsaturated, the model assumes continuous infiltration, overlooking the threshold effects of saturation-excess runoff. Consequently, the model underperforms during initial rainfall and prolonged rain events. For example, under pre-event drought conditions, the model may allocate all early rainfall to infiltration, delaying or underestimating the flood peak. Furthermore, the model is highly sensitive to infiltration-related parameters, requiring accurate calibration of initial infiltration rate, infiltration decay coefficients, and others. However, infiltration capacity in the Juma River basin is heavily influenced by antecedent soil moisture conditions (e.g., low water absorption in dry soils), complicating parameter calibration and undermining the reliability of flood forecasting.

In different climatic regions—particularly under short-duration, high-intensity rainfall—both saturation-excess and infiltration-excess mechanisms may coexist within small watersheds. Since a single runoff generation mechanism cannot fully capture the diverse rainfall-runoff responses of various basins, it is difficult to establish an accurate quantitative relationship using a single model type (Zhai et al., 2020). The geographic and climatic conditions of the Juma River basin may cause saturation-excess runoff to occur rapidly at the onset of rainfall, While infiltration-excess runoff can also occur during localized downpours—conceptually, for example, when hourly rainfall exceeds 30 mm and surpasses the soil's infiltration capacity even if the soil is not saturated—this threshold is used illustratively here unless specific regional studies inform it. The generally good performance of the Xin'anjiang model (XAJ), particularly in capturing the initial rising limb and peak timing for many events, suggests that saturation-excess runoff, driven by rising water tables in shallow soils, is a dominant mechanism in the Juma basin. However, occasional underestimations during very intense, short-duration rainfall within larger events might hint at challenges in fully capturing localized infiltration-excess contributions, suggesting a potential co-existence or temporal shift in dominant mechanisms under specific storm characteristics. Therefore, a model capable of handling both mechanisms simultaneously is needed to accommodate the spatial and temporal variability of rainfall in the Juma River basin, particularly under conditions such as early drought followed by intense, concentrated rainfall.

5 Conclusion

Based on precipitation and evaporation data from 1955 to 2019 in the upper reaches of the Juma River basin, this study employed the Xin'anjiang Model, the Vertical Mixed Runoff Generation Model, and the Dahuofang Model to analyze representative flood events in the region. Using a standardized flood forecasting evaluation methodology, the simulation accuracy and relevant performance indicators of each model under identical flood scenarios were compared to assess their applicability and forecasting capabilities. The main conclusions are as follows:

(1) Compared to the Vertical Mixed Runoff Generation Model and the Dahuofang Model, the Xin'anjiang Model demonstrates better agreement between simulated and observed flood processes in the upper Juma River basin, indicating that it is more suitable for application in this region.
(2) The forecasting indicators of the Xin'anjiang Model meet the required technical standards: the relative errors of simulated

flood volume and peak discharge are both below 20%; the average absolute error of peak time occurrence is 0.47 h; and the average Nash-Sutcliffe Efficiency Coefficient reaches 0.69. These results indicate that the model is applicable for operational hydrological forecasting in the upper Juma River basin.

(3) All three runoff generation models perform better in simulating single-peaked floods compared to multi-peaked ones, with improved simulation accuracy observed for larger-magnitude single-peaked floods.

Due to limitations in available flood data, a complete flood validation process could not be conducted strictly in accordance with hydrological forecasting standards. Moreover, the selected flood events spanned a long time period during which the basin underwent large-scale management, leading to significant changes in the underlying surface conditions and affecting the basin's storage and regulation capacity (Wang et al., 2021; Li et al., 2012). For instance, significant changes in land use (e.g., urbanization expanding impervious areas) could alter runoff generation rates and concentration times, while new or modified water management structures (e.g., reservoirs or diversion channels) could directly modify flow regimes. Such changes might impact the stationarity of calibrated model parameters over long periods, potentially requiring model recalibration or structural adjustments to maintain forecast accuracy. Future efforts should prioritize acquiring data from recent major floods (e.g., post-2019 events including the 2023 Haihe flood) for model validation under potentially evolving contemporary conditions. Furthermore, investigating adaptive parameterization techniques or ensemble multi-model approaches could be beneficial to account for long-term basin changes and the nuanced interplay of different runoff generation mechanisms (Wu et al., 2020).

Data availability statement

The data analyzed in this study is subject to the following licenses/restrictions: Data available on request due to privacy. Requests to access these datasets should be directed to Fuxin Chai, chaifx@iwhr.com.

Author contributions

TL: Writing – review & editing, Writing – original draft. SH: Writing – review & editing. FC: Writing – review & editing, Supervision. KL: Writing – review & editing. HT: Writing – review & editing.

Funding

The author(s) declare that no financial support was received for the research and/or publication of this article.

Conflict of interest

The authors declare that the research was conducted in the absence of any commercial or financial relationships that could be construed as a potential conflict of interest.

The reviewer WW declared a shared affiliation with the authors (TL, SH, and HT) to the handling editor at the time of review.

Generative AI statement

The authors declare that no Gen AI was used in the creation of this manuscript.

Publisher's note

References

Awol, F. S., Coulibaly, P., and Tsanis, I. (2021). Identification of combined hydrological models and numerical weather predictions for enhanced flood forecasting in a Semiurban watershed. *J. Hydrol. Eng.* 26:26. doi: 10.1061/(ASCE)HE.1943-5584.0002018

Birkmann, J., Cutter, S. L., Rothman, D. S., Welle, T., Garschagen, M., van Ruijven, B., et al. (2015). Scenarios for vulnerability: opportunities and constraints in the context of climate change and disaster risk. *Clim. Chang.* 133, 53–68. doi: 10.1007/s10584-013-0913-2

Che, Y. Z. (2024). Application of Xinan River model in Zijingguan River basin. *Heilongjiang Hydraulie Sci. Technol.* 52, 90–93.

Chen, Y., Li, J., and Xu, H. (2016). Improving flood forecasting capability of physically based distributed hydrological models by parameter optimization. *Hydrol. Earth Syst. Sci.* 20, 375–392. doi: 10.5194/hess-20-375-2016

Chen, D., Pan, C., Qiao, S., Zhi, R., Tang, S., Yang, J., et al. (2023). Evolution and prediction of the extreme rainstorm event in July 2021 in Henan province, China. *Atmos. Sci. Lett.* 24:1156. doi: 10.1002/asl.1156

Chen, Y., Zhang, N., Zhang, X., Wang, G., Wang, Y., Liu, R., et al. (2025). A novel dynamic flash flood early warning framework based on distributed hydrologic modeling. *Ecol. Indic.* 172:113247. doi: 10.1016/j.ecolind.2025.113247

Compilation group of China Flood and Drought Disaster Prevention Bulletin (2023). Summary of China flood and drought disaster prevention bulletin 2022. *China Flood Drought Manag.* 33, 78–82. doi: 10.16867/j.issn.1673-9264.2023410

Duan, W., He, B., Nover, D., Fan, J., Yang, G., Chen, W., et al. (2016). Floods and associated socioeconomic damages in China over the last century. *Nat. Hazards* 82, 401–413. doi: 10.1007/s11069-016-2207-2

Emerton, R. E., Stephens, E. M., Pappenberger, F., Pagano, T. C., Weerts, A. H., Wood, A. W., et al. (2016). Continental and global scale flood forecasting systems. *Wires Water* 3, 391–418. doi: 10.1002/wat2.1137

Grimaldi, S., Schumann, G. J., Shokri, A., Walker, J. P., and Pauwels, V. R. N. (2019). Challenges, opportunities, and pitfalls for global coupled hydrologic-hydraulic modeling of floods. *Water Resour. Res.* 55, 5277–5300. doi: 10.1029/2018WR024289

Jain, S. K., Mani, P., Jain, S. K., Prakash, P., Singh, V. P., Tullos, D., et al. (2018). A brief review of flood forecasting techniques and their applications. *Int. J. River Basin Manag.* 16, 329–344. doi: 10.1080/15715124.2017.1411920

Jin, H., Rui, X., and Li, X. (2022). Analysing the performance of four hydrological models in a Chinese arid and semi-arid catchment. *Sustain. For.* 14:677. doi: 10.3390/su14063677

Kimuli, J. B., Di, B., Zhang, R., Wu, S., Li, J., and Yin, W. (2021). A multisource trend analysis of floods in Asia-Pacific 1990–2018: implications for climate change in sustainable development goals. *Int. J. Disaster Risk Reduct.* 59:102237. doi: 10.1016/j.ijdrr.2021.102237

Kumar, V., Azamathulla, H. M., Sharma, K. V., Mehta, D. J., and Maharaj, K. T. (2023). The state of the art in deep learning applications, challenges, and future prospects: a

comprehensive review of flood forecasting and management. *Sustain. For.* 15:543. doi: 10.3390/su151310543

Kumar, V., Sharma, K. V., Caloiero, T., Mehta, D. J., and Singh, K. (2023). Comprehensive overview of flood modeling approaches: a review of recent advances. *Hydrology* 10:141. doi: 10.3390/hydrology10070141

Kundzewicz, Z. W., Huang, J., Pinskwar, I., Su, B., Szwed, M., and Jiang, T. (2020). Climate variability and floods in China - a review. *Earth-Sci. Rev.* 211:103434. doi: 10.1016/j.earscirev.2020.103434

Lan, L., and Wang, X. (2025). Large-scale flood mapping using Sentinel-1 and Sentinel-2 imagery: spatio-temporal analysis of the 23·7 Haihe basin-wide extreme flood. *J. Hydrol.* 653:132777. doi: 10.1016/j.jhydrol.2025.132777

Li, Z. J., Yu, S. S., Dai, J. N., Yao, Y. M., Zhang, J. Z., Hu, C. Q., et al. (2012). Research on influences of underlaying surface changes to the floods based on hydrological model. *Yellow River* 34, 17–19.

Lu, M. J. (2021). Recent and future studies of the Xinanjiang model. *Shuili Xuebao* 52, 432–441.

Ma, Q., Wang, Y., Wei, L., Shi, C. X., Wang, H. W., Zhang, X. X., et al. (2024). A modelling-based assessment approach of basin flood spatiotemporal characteristics. *Adv. Water Sci.* 35, 726–737.

Mai, T., Mushtaq, S., Reardon-Smith, K., Webb, P., Stone, R., Kath, J., et al. (2020). Defining flood risk management strategies: a systems approach. *Int. J. Disaster Risk Reduct.* 47:101550. doi: 10.1016/j.ijdrr.2020.101550

Mathevet, T., Michel, C., Andréassian, V., and Perrin, C. (2006). A bounded version of the Nash-Sutcliffe criterion for better model assessment on large sets of basins. *Iahs Aish Publication* 307, 211–219.

Nie, Y., and Sun, J. (2022). Moisture sources and transport for extreme precipitation over Henan in July 2021. *Geophys. Res. Lett.* 49:7446. doi: 10.1029/2021GL097446

Qi, W., Ma, C., Xu, H., Chen, Z., Zhao, K., and Han, H. (2021). A review on applications of urban flood models in flood mitigation strategies. *Nat. Hazards* 108, 31–62. doi: 10.1007/s11069-021-04715-8

Ran, J., and Nedovic-Budic, Z. (2016). Integrating spatial planning and flood risk management: a new conceptual framework for the spatially integrated policy infrastructure. *Comput. Environ. Urban. Syst.* 57, 68–79. doi: 10.1016/j.compenvurbsys.2016.01.008

Rehman, J., Sohaib, O., Asif, M., and Pradhan, B. (2019). Applying systems thinking to flood disaster management for a sustainable development. *Int. J. Disaster Risk Reduct.* 36:101101. doi: 10.1016/j.ijdrr.2019.101101

Ren-Jun, Z. (1992). The Xinanjiang model applied in China. *J Hydrol (Amst)* 135, 371–381. doi: 10.1016/0022-1694(92)90096-E

Sam, A. S., Abbas, A., Surendran Padmaja, S., Raghavan Sathyan, A., Vijayan, D., Kächele, H., et al. (2021). Flood vulnerability and food security in eastern India: a threat to the achievement of the sustainable development goals. *Int. J. Disaster Risk Reduct.* 66:102589. doi: 10.1016/j.ijdrr.2021.102589

Wang, Y., Wang, W., Xu, D., Zhao, Y., and Zang, H. (2024). A novel strategy for flood flow prediction: integrating spatio-temporal information through a two-dimensional hidden layer structure. *J. Hydrol.* 638:131482. doi: 10.1016/j.jhydrol.2024.131482

Wang, Q., Xu, Y., Cai, X., Tang, J., and Yang, L. (2021). Role of underlying surface, rainstorm and antecedent wetness condition on flood responses in small and medium sized watersheds in the Yangtze River Delta region, China. *Catena* 206:105489. doi: 10.1016/j.catena.2021.105489

Wang, X., Zhai, X., Zhang, Y., and Guo, L. (2023). Evaluating flash flood simulation capability with respect to rainfall temporal variability in a small mountainous catchment. *J. Geogr. Sci.* 33, 2530–2548. doi: 10.1007/s11442-023-2188-5

Wang, W., Zhao, Y., Chau, K., Xu, D., and Liu, C. (2021). Improved flood forecasting using geomorphic unit hydrograph based on spatially distributed velocity field. *J. Hydroinf.* 23, 724–739. doi: 10.2166/hydro.2021.135

Wee, G., Chang, L., Chang, F., and Mat Amin, M. Z. (2023). A flood impact-based forecasting system by fuzzy inference techniques. *J. Hydrol.* 625:130117. doi: 10.1016/j.jhydrol.2023.130117

Wu, W., Emerton, R., Duan, Q., Wood, A. W., Wetterhall, F., and Robertson, D. E. (2020). Ensemble flood forecasting: current status and future opportunities. *Wires Water* 7:1432. doi: 10.1002/wat2.1432

Xu, Z. X. (2010). Hydrological models: past present and future. *J. Beijing Normal Univ.* 46, 278–289.

Ye, J. Y., Wu, Y. T., Li, Z. J., and Chang, L. (2012). Forecasting methods for flash floods in medium and small rivers in humid regions and their applications. *J. Hohai Univ.* 40, 615–621.

Zhai, X. Y., Guo, L., Liu, R. H., Zhang, Y. Y., and Liu, C. J. (2020). Development and application of China flash flood hydrological model: case study in small and medium-sized catchments of Anhui Province. *J. Basic Sci. Eng.* 28, 1018–1036.

Zhai, X., Guo, L., Liu, R., Zhang, Y., and Zhang, Y. (2021). Comparing three hydrological models for flash flood simulations in 13 humid and semi-humid mountainous catchments. *Water Resour. Manag.* 35, 1547–1571. doi: 10.1007/s11269-021-02801-x

Zhai, X., Zhang, Y., Zhang, Y., Guo, L., and Liu, R. (2021). Simulating flash flood hydrographs and behavior metrics across China: implications for flash flood management. *Sci. Total Environ.* 763:142977. doi: 10.1016/j.scitotenv.2020.142977

Zhang, Q., and Wang, Y. (2022). Distribution of hazard and risk caused by agricultural drought and flood and their correlations in summer monsoon–affected areas of China. *Theor. Appl. Climatol.* 149, 965–981. doi: 10.1007/s00704-022-04093-6

Zhao, X., Li, H., Cai, Q., Pan, Y., and Qi, Y. (2023). Managing extreme rainfall and flooding events: a case study of the 20 July 2021 Zhengzhou flood in China. *Climate* 11:228. doi: 10.3390/cli11110228

Zhu, J. M., and Zhou, M. C. (2016). Comparative application of different hydraulic models in Shuanggiao Basin. *Yellow River* 38, 22–26.